Extended Disturbance-Observer-Based Data-Driven Control of Networked Nonlinear Systems With Event-Triggered Output

Mouquan Shen, Xianming Wang, Ju H. Park, *Senior Member, IEEE*, Yang Yi, and Wei-Wei Che

***Abstract*—This article is dedicated to data-driven control of networked nonlinear systems with event-triggered output. An improved extended state observer is constructed to estimate unknown disturbances. An output estimator is built on the triggered output and the estimated output. Consequently, triggering conditions for single-input single-output and multiple-inputs and multiple-outputs systems are individually proposed by integrating the estimated disturbances, the true and the estimated tracking errors. Sufficient conditions are established to guarantee that the resultant tracking error systems are uniformly ultimately bounded. The proposed strategies are verified by illustrative numerical examples.**

***Index Terms*—Data-driven control (DDC), dynamic linearization, event-triggered (ET) control.**

I. Introduction

ENJOYING the attractive features of reducing physical wiring, simplified maintenance, and increasing flexibility, much attention has been devoted to networked control systems not only on theory but also for practical applications [1], [2], [3], [4], [5]. Usually, periodical sampling has been frequently employed to coordinate digital signal transmission [5]. While this sampling method is readily implemented, unnecessary transmission occupies limited bandwidth when systems run at equilibrium points. Consequently, system performance could be deteriorated by packet dropouts [6], time delays [7], fading channels [8], and so on. As an alternative solution, event-triggered (ET) control comes into the sight of researchers since transmissions are determined by the prescribed triggering rules [9], [10], [11], [12]. Around this topic, fruitful ET results have been reported in [13], [14], and [15]. Particularly, the input to state stability is employed by [13] to get an absolute triggering measurement. In [14], a periodical ET strategy is built on the conventional periodic sampling-data control and ET control to get a minimum interevent time for global exponential stability of impulsive systems, piecewise linear systems, and perturbed linear systems, respectively. Gu et al. [15] proposed an adaptive ET condition for networked nonlinear interconnected systems. It should be pointed out that system models in most of the above mentioned results are known beforehand. Moreover, Lyapunov functions adopted to stability analysis for triggered closed-loop systems are required to decrease monotonically.

Due to inherent unmodeled dynamics, it is hard to meet the dependency on the system model [16], [17], [18]. Therefore, data-driven control (DDC) methods are widely adopted to construct control schemes. Until now, some representative DDC strategies have been proposed, such as model free adaptive control (MFAC), data-based control [19], lazy learning control [20]. Among them, MFAC has been favored by [21], [22], and [23] since it needs less computational cost. Consequently, the established ET rules with perfect system models should be reconsidered in the MFAC framework. Regarding to ET MFAC, [24] provides ET mechanisms for compact form, partial form, and full form, respectively. Along this line, the Lyapunov-like method is exploited by [25] and [26] to get an ET model-free iterative learning control (ETMFILC) for repetitive nonaffine nonlinear systems. Different from [24], [25], and [26], an adaptive ET mode is developed by [27] with the help of neural network (NN) to estimate pseudo-gradient vector. Although the aforementioned results have contributed to the research on ET MFAC, attention is only paid to the mechanism on system inputs. On the other hand, multifaceted disturbances may deteriorate the performance of modern industry processes [28], [29], [30]. To attenuate their influence, a NN-based disturbance observer is established in [28] for disturbed nonlinear systems. Albeit this observer could perform powerful capability of adaptability and tackling nonlinearity, heavy computation is unavailable [29]. To

Manuscript received 26 August 2022; revised 8 November 2022; accepted 10 November 2022. Date of publication 29 November 2022; date of current version 17 April 2023. The work of Mouquan Shen, Yang Yi, and Wei-Wei Che was supported in part by the National Natural Science Foundation of China under Grant 62173177, Grant 62273254, Grant 61773200, Grant U1966202, Grant 61873338, and Grant 61973266; in part by the Postgraduate Research and Practice Innovation Program of Jiangsu Province; and in part by the Taishan Scholars under Grant tsqn201812052. The work of Ju H. Park was supported by the National Research Foundation of Korea (NRF) Grant funded by the Korea Government (Ministry of Science and ICT) under Grant 2019R1A5A8080290. This article was recommended by Associate Editor X. Ge. *(Corresponding authors: Mouquan Shen; Ju H. Park.)*

Mouquan Shen is with the College of Electrical Engineering and Control Science, Nanjing Tech University, Nanjing 211816, China, and also with the Department of Electrical Engineering, Yeungnam University, Gyeongsan 38541, Republic of Korea (e-mail: shenmouquan@njtech.edu.cn).

Xianming Wang is with the School of Mechanical and Power Engineering, Nanjing Tech University, Nanjing 211816, China (e-mail: wangxianming@njtech.edu.cn).

Ju H. Park is with the Department of Electrical Engineering, Yeungnam University, Gyeongsan 38541, Republic of Korea (e-mail: jessie@ynu.ac.kr).

Yang Yi is with the Department of Automation, School of Information Engineering, Yangzhou University, Yangzhou 225127, China (e-mail: yiyang@yzu.edu.cn).

Wei-Wei Che is with the Institute of Complexity Science, Qingdao University, Qingdao 266071, China (e-mail: cwwemail1980@126.com).

Color versions of one or more figures in this article are available at https://doi.org/10.1109/TSMC.2022.3222491.

Digital Object Identifier 10.1109/TSMC.2022.3222491

treat this issue, [30] explores an extended state observer (ESO) to estimate unknown nonlinearities for nonaffine nonlinear discrete-time systems. It should be pointed out that the above results just focus on either ET strategies or disturbance compensation. However, combining them together cannot be treated the ET output model free iterative learning control (MFILC) with unknown disturbances in this article. Moreover, the observer configuration in [30] still has room to be further improved.

Motivated by the above observations, this article is devoted to output-based ETMFILC under ESO strategy for disturbed nonlinear discrete-time systems. Distinguished from the ESO in [30], an improved version with extra parameter is proposed to treat the output ET case and reduce observation error boundary. Based on the modified ESO, an output dynamic estimator is supplied to update the MFILC schemes with periodic outputs and applied as compensator for the ESO. Consequently, output ET strategies integrating the estimated disturbances, the true tracking errors, and the estimated errors are presented by means of the Lyapunov method for single-input single-output (SISO) and multiple-inputs and multiple-outputs (MIMO) systems, respectively. With the proposed ETMFILC schemes, the uniformly ultimately bounded error systems are established for two scenarios. Illustrative examples are supplied to demonstrate the validity of the presented methods. In summary, compared with existing results, the contributions are collected as following points.

1) An improved ESO configuration is constructed to treat output ET case and reduce observation error boundary.
2) Output-based ETMFILC schemes are established to reduce communication transmissions and enhance disturbance attenuation.

The following organization has five parts. Section II provides problem formulation. ETMFILC schemes for both SISO and MIMO systems are detailed in Section III. In Section IV, the validity of the proposed schemes for SISO and MIMO systems is verified by two examples. Conclusion with some future research topics is supplied in Section V.

Notations: B^{T} denotes the transposition of B. Δ means backward difference. $\|\cdot\|_p$ is induced consistent norm and $\|\cdot\|_v$ is the consistent norm. $\|\cdot\|$ is the 2-norm, $|\cdot|$ represents the absolute value operation and $P_{j=a}^{b} s_j = s_a \cdot s_{a+1}, \ldots, s_b$.

II. Problem Formulation

Consider a class of repetitive nonlinear discrete-time system with disturbance as

$$\begin{aligned} y_k(\iota+1) = f\big(&y_k(\iota), \ldots, y_k\big(\iota - c_y\big) \\ &u_k(\iota), \ldots, u_k(\iota - c_u)) + d_k(\iota) \end{aligned} \tag{1}$$

where $y_k(\iota) \in \mathcal{R}^m$, $u_k(\iota) \in \mathcal{R}^m$, $d_k(\iota) \in \mathcal{R}^m$ represent output, input, and disturbance, respectively. $k \in \{0, 1, 2, \ldots\}$ is iteration index and $\iota \in \{0, 1, \ldots, T\}$ is sampling instant. c_y and c_u are unknown positive constants, $f(\cdot) \in \mathcal{R}^m$ is a nonlinear function.

To proceed, assumptions and a lemma are given first.

Assumption 1 [25]: The partial derivative of $f(\cdot)$ with respect to $u_k(\iota)$ is continuous in the direction of iteration.

Assumption 2 [25]: System (1) meets Lipschitz condition in iteration direction, which means $\|\Delta y_k(\iota+1)\| \le b\|\Delta u_k(\iota)\|$ with $\|\Delta u_k(\iota)\| \neq 0$, where $\Delta y_k(\iota+1) = y_k(\iota+1) - y_{k-1}(\iota+1)$, $\Delta u_k(\iota) = u_k(\iota) - u_{k-1}(\iota)$, and b is a unknown positive constant.

Assumption 3: The input change for (1) is limited by

$$\|u_k(\iota) - u_k(\iota-1)\| \le b_{\Delta u} \tag{2}$$

where $b_{\Delta u}$ is a unknown positive constant.

Remark 1: As [30], (2) is employed to ensure the boundedness of observation errors in Theorems 2 and 5, respectively. In engineering sense, it is utilized to prevent input chattering against damaging the controller, such as high wear of moving mechanical parts [31] and high heat losses of power circuits [32].

Lemma 1 [28]: Under Assumptions 1 and 2, system (1) is transformed into a compact model

$$\Delta y_k(\iota+1) = \Psi_k(\iota)\Delta u_k(\iota) + \xi_k(\iota) \tag{3}$$

where $\|\Psi_k(\iota)\| \le b$ is called pseudo partial derivative (PPD) and $\|\xi_k(\iota)\| \le b_\xi$ denotes system uncertainties. Additionally, b_ξ is a unknown positive constant.

Remark 2: Equation (3) describes the mapping between system inputs and outputs without physical meanings. Similar to [16], $\Psi_k(\iota)$ is required to change slowly at iteration direction so that it is insensitive to the iteration-varying factors.

Remark 3: Like (3), a full case can be obtained by replacing $\Psi_k(\iota) = [(\partial f(\cdot)/\partial y_k(\iota)), \ldots, (\partial f(\cdot)/\partial y_{k-l_y+1}(\iota)), (\partial f(\cdot)/\partial u_k(\iota)), \ldots, (\partial f(\cdot)/\partial u_{k-l_u+1}(\iota))]$, $\Delta u_k(\iota) = [\Delta y_k^{\mathrm{T}}(\iota), \ldots, \Delta y_{k-l_y+1}^{\mathrm{T}}(\iota), \Delta u_k^{\mathrm{T}}(\iota), \ldots, \Delta u_{k-l_u+1}^{\mathrm{T}}(\iota)]^{\mathrm{T}}$, and $\xi_k(\iota) = f(y_{k-l_y}(\iota), y_k(\iota-1), \ldots, y_k(\iota-c_y), u_{k-l_u}(\iota), u_k(\iota-1), \ldots, u_k(\iota-c_u)) - f(y_{k-1}(\iota), \ldots, y_{k-1}(\iota-c_y), u_{k-1}(\iota), \ldots, u_{k-1}(\iota-c_u)) + \Delta d_k(\iota)$, where l_y and $l_u \in \{1, 2\cdots\}$.

Lemma 2 [33]: Denote $\mathrm{S}(A)$ as the spectral radius of matrix $A \in R^{n\times n}$. There is an induced consistent norm $\|\cdot\|_p$ that makes $\|A\|_p \le \mathrm{S}(A) + \epsilon$ ($\epsilon > 0$).

To facilitate the observer construction, set $g_k(\iota) = [\bar{g}_k(\iota), \bar{\bar{g}}_k(\iota)]^{\mathrm{T}} = [y_k(\iota), \xi_k(\iota)]^{\mathrm{T}}$. Therefore, (3) is rewritten as

$$\begin{cases} \bar{g}_k(\iota+1) = \bar{g}_k(\iota) + \Psi_k(\iota)(u_k(\iota) - u_k(\iota-1)) \\ \quad +\bar{\bar{g}}_k(\iota) \\ \bar{\bar{g}}_k(\iota+1) = \xi_k(\iota+1). \end{cases} \tag{4}$$

Inspired by [30], an improved ESO is built as follows:

$$\begin{cases} \hat{\bar{g}}_k(\iota+1) = \hat{\bar{g}}_k(\iota) + \hat{\bar{\bar{g}}}_k(\iota) + \hat{\Psi}_k(\iota)(u_k(\iota) - u_k(\iota-1)) \\ \quad +l_1\Big(\bar{g}_k(\iota) - \hat{\bar{g}}_k(\iota)\Big) \\ \hat{\bar{\bar{g}}}_k(\iota+1) = l_3\hat{\bar{\bar{g}}}_k(\iota) + l_2\Big(\bar{g}_k(\iota) - \hat{\bar{g}}_k(\iota)\Big) \end{cases} \tag{5}$$

where $\hat{\bar{g}}_k(\iota)$ and $\hat{\bar{\bar{g}}}_k(\iota)$ are adopted to estimate $\bar{g}_k(\iota)$ and $\bar{\bar{g}}_k(\iota)$, respectively. l_1, l_2, and l_3 are positive scalar selected by designers to meet $0 < l_1 < 1$, $0 < l_3 < 1$ and

$$\begin{aligned} \bar{\theta} = \max\Bigg\{ &\Bigg|\frac{1 + l_3 - l_1 + \sqrt{(l_1 - l_3 - 1)^2 - 4(l_3 + l_2 - l_1 l_3)}}{2}\Bigg| \\ &\Bigg|\frac{1 + l_3 - l_1 - \sqrt{(l_1 - l_3 - 1)^2 - 4(l_3 + l_2 - l_1 l_3)}}{2}\Bigg|\Bigg\} < 1. \end{aligned} \tag{6}$$

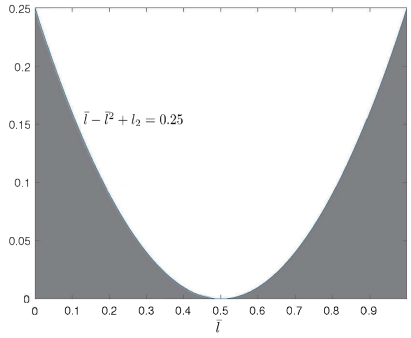

Fig. 1. Selection range of parameters.

In order to reduce the computational complexity, without loss generality, selecting $\bar{l} = l_1 = l_3 \in (0, 0.5) \cup (0.5, 1)$ such that $\bar{l} - \bar{l}^2 + l_2 < 0.25$ holds. Moreover, Fig. 1 is provided to show their relationship. In the simulation, a possible choice is $\bar{l} = 0.1$ and $l_2 = 0.01$.

Remark 4: Compared with [30], an extra l_3 is introduced to not only treat the output ET case but also reduce observation error boundary.

Borrowed from [28], the MFILC scheme for periodical outputs is presented as

$$\hat{\Psi}_{k+1}(\iota) = \hat{\Psi}_k(\iota) + \frac{\eta W_k(\iota)\Delta u_k(\iota)}{\mu + \Delta u_k(\iota)^2} \tag{7}$$

$$u_{k+1}(\iota) = u_k(\iota) + \frac{\rho\hat{\Psi}_{k+1}(\iota)\left[e_k(\iota+1) - \hat{\bar{\bar{g}}}_{k+1}(\iota)\right]}{\lambda + \left\|\hat{\Psi}_{k+1}(\iota)\right\|^2} \tag{8}$$

where $W_k(\iota) = \Delta y_k(\iota+1) - \hat{\Psi}_k(\iota)\Delta u_k(\iota)$, the true tracking error $e_k(\iota+1) = y^*(\iota+1) - y_k(\iota+1)$, $y^*(\iota+1)$ denotes the desired output and the choices of η, μ, ρ, and λ meets $0 < \eta < 1$, $\mu > 0$, $0 < \rho < 1$, and $\lambda > 0$, respectively.

This article aims to update (7) and (8) with ET output. To realize this aim, an ET sequence is first defined as $\{k_l\}$, $l = 1, 2, \ldots, N$. Then $\hat{\Psi}_k(\iota)$ is updated by

$$\hat{\Psi}_{k+1}(\iota) = \begin{cases} \hat{\Psi}_k(\iota) + \dfrac{\eta W_k(\iota)\Delta u_k(\iota)}{\mu + \|\Delta u_k(\iota)\|^2}, & k = k_l \\ \hat{\Psi}_k(\iota), & k_l < k < k_{l+1} \end{cases} \tag{9}$$

$$\hat{\Psi}_k(\iota) = \hat{\Psi}_1(1), \text{ if } |\hat{\Psi}_k(\iota)| < \omega \text{ or } |\Delta u_{k-1}(\iota)| < \omega \text{ or } \operatorname{sign}\left(\hat{\Psi}_k(\iota)\right) \neq \operatorname{sign}\left(\hat{\Psi}_1(1)\right) \tag{10}$$

and $u_{k+1}(\iota)$ is reconstructed as

$$u_{k+1}(\iota) = \begin{cases} u_k(\iota) + \dfrac{\rho\hat{\Psi}_{k+1}(\iota)\left[e_k(\iota+1) - \hat{\bar{\bar{g}}}_{k+1}(\iota)\right]}{\lambda + \hat{\Psi}_{k+1}(\iota)^2}, & k = k_l \\ u_k(\iota) + \dfrac{\rho\hat{\Psi}_{k+1}(\iota)\left[\hat{e}_k(\iota+1) - \hat{\bar{\bar{g}}}_{k+1}(\iota)\right]}{\lambda + \hat{\Psi}_{k+1}(\iota)^2}, & k_l < k < k_{l+1} \end{cases} \tag{11}$$

where $\hat{\Psi}_1(1)$ is the initial value of $\hat{\Psi}_k(\iota)$, ω is an arbitrarily small positive constants, $\hat{e}_k(\iota+1) = y^*(\iota+1) - \hat{y}_k(\iota+1)$ and $\hat{y}_k(\iota+1)$ is driven by an output dynamic estimator as

$$\hat{y}_k(\iota) = \begin{cases} y_k(\iota-1) + \Upsilon_k(\iota-1), & k = k_l \\ \hat{y}_k(\iota-1) + \Upsilon_k(\iota-1), & k_l < k < k_{l+1} \end{cases} \tag{12}$$

where $\Upsilon_k(\iota-1) = \hat{\Psi}_k(\iota-1)(u_k(\iota-1) - u_k(\iota-2)) + \hat{\bar{\bar{g}}}_k(\iota-1)$.

Remark 5: In (11), a large input increment is avoided by introducing λ so that the constraint (2) is satisfied.

Remark 6: Note that $\hat{y}_k(\iota)$ under (12) is composed of $\hat{\Psi}_k(\iota-1)$ and $\hat{\bar{\bar{g}}}_k(\iota-1)$. Moreover, the estimation error boundary of $\hat{\Psi}_k(\iota-1)$ and $\hat{\bar{\bar{g}}}_k(\iota-1)$ determined by η, μ, l_1, l_2, and l_3 is presented in subsequent Theorems 1 and 2. Therefore, adjusting these parameters could make $\tilde{y}_k(\iota) = y_k(\iota) - \hat{y}_k(\iota)$ be small enough.

With the estimated $y_k(\iota)$, the ET ESO is given as

$$\begin{cases} \begin{cases} \hat{\bar{g}}_k(\iota+1) = \hat{\bar{g}}_k(\iota) + \hat{\bar{\bar{g}}}_k(\iota) + \hat{\Psi}_k(\iota)(u_k(\iota) - u_k(\iota-1)) \\ \quad + l_1\left(\bar{g}_k(\iota) - \hat{\bar{g}}_k(\iota)\right) \\ \hat{\bar{\bar{g}}}_k(\iota+1) = l_3\hat{\bar{\bar{g}}}_k(\iota) + l_2\left(\bar{g}_k(\iota) - \hat{\bar{g}}_k(\iota)\right), \quad k = k_l \end{cases} \\ \begin{cases} \hat{\bar{g}}_k(\iota+1) = \hat{\bar{g}}_k(\iota) + \hat{\bar{\bar{g}}}_k(\iota) + \hat{\Psi}_k(\iota)(u_k(\iota) - u_k(\iota-1)) \\ \quad + l_1\left(\hat{y}_k(\iota) - \hat{\bar{g}}_k(\iota)\right) \\ \hat{\bar{\bar{g}}}_k(\iota+1) = l_3\hat{\bar{\bar{g}}}_k(\iota) + l_2\left(\hat{y}_k(\iota) - \hat{\bar{g}}_k(\iota)\right), \quad k_l < k < k_{l+1} \end{cases} \end{cases} \tag{13}$$

and the triggering error $e_{ETk}(\iota)$ is presented as

$$e_{ETk}(\iota) = y_k(\iota) - \hat{y}_k(\iota). \tag{14}$$

III. Main Results

This section is concentrated on triggering mechanisms design and boundedness proof of PPD estimation error, observation error, and tracking error for SISO and MIMO systems, respectively.

A. SISO System

Resorting to the above preliminaries, the proposed triggering mechanism is

$$D\left(R(\cdot)\right) > e_k^2(\iota+1) \tag{15}$$

where $R(\cdot) = [(1-\upsilon)e_k(\iota+1) - \upsilon e_{ETk}(\iota+1) - (1-\upsilon)\hat{\bar{\bar{g}}}_{k+1}(\iota)]^2$, $\upsilon = \rho\hat{\Psi}_{k+1}^2(\iota)/(\lambda + \hat{\Psi}_{k+1}^2(\iota))$, $D(R(\cdot))$ is a dead-zone operator as follows:

$$D\left(R(\cdot)\right) = \begin{cases} R(\cdot), & \text{if } |e_k(\iota+1)| > H_e \\ 0, & \text{otherwise} \end{cases} \tag{16}$$

where H_e is a positive constant selected by the designers.

Remark 7: By integrating (15), the estimated $\hat{\bar{\bar{g}}}_{k+1}(\iota)$ is designed by employing the Lyapunov method. Actually, the mechanism may be not triggered once the estimation error falls into the prescribed performance interval. Moreover, Zeno behavior could be avoided by the designed dead-zone operator (16).

Consequently, the output-based ETMFILC scheme is summarized as (9)–(16).

Now it is the position to analyze that PPD estimation error $\tilde{\Psi}_{k+1}(\iota)$ is uniformly ultimately bounded under ETMFILC for SISO system.

Theorem 1: If the system (1) meets Assumptions 1–3 and select η and μ meeting $0 < \eta < 1$ and $\mu > 0$, $\tilde{\Psi}_{k+1}(\iota)$ under the triggering scheme (9)–(16) converges to $(\Theta/1 - M_3)$, where $\Theta = (\eta b_\xi/2\sqrt{\mu})$ and $0 < M_3 < 1$.

Proof: From (9), $\hat{\Psi}_k(\iota)$ remains unchanged when (15) is not violated, i.e., $k_l < k < k_{l+1}$. Therefore, just pay attention to $\hat{\Psi}_k(\iota)$ at the triggered iterations ($k = k_l$).

If $|\hat{\Psi}_k(\iota)| < \omega$, the boundedness of $\hat{\Psi}_k(\iota)$ is guaranteed by the reset algorithm (10). Otherwise, choosing $\tilde{\Psi}_k(\iota) = \hat{\Psi}_k(\iota) - \Psi_k(\iota)$ and subtracting $\Psi_{k+1}(\iota)$ on both sides of (9) yields

$$\tilde{\Psi}_{k+1}(\iota) = \left(1 - \frac{\eta \Delta u_k^2(\iota)}{\mu + \Delta u_k^2(\iota)}\right)\tilde{\Psi}_k(\iota) + \frac{\eta \xi_k(\iota)\Delta u_k(\iota)}{\mu + \Delta u_k^2(\iota)} + \Psi_k(\iota) - \Psi_{k+1}(\iota). \tag{17}$$

Resorting to Remark 2, (17) is rewritten as

$$\tilde{\Psi}_{k+1}(\iota) = \left(1 - \frac{\eta \Delta u_k^2(\iota)}{\mu + \Delta u_k^2(\iota)}\right)\tilde{\Psi}_k(\iota) + \frac{\eta \xi_k(\iota)\Delta u_k(\iota)}{\mu + \Delta u_k^2(\iota)}. \tag{18}$$

Recalling Lemma 1 gives

$$\left|\frac{\eta \xi_k(\iota)\Delta u_k(\iota)}{\mu + \Delta u_k^2(\iota)}\right| \le \frac{\eta |\xi_k(\iota)||\Delta u_k(\iota)|}{2\sqrt{\mu}|\Delta u_k(\iota)|} \le \frac{\eta b_\xi}{2\sqrt{\mu}}. \tag{19}$$

Substituting (19) into (18) provides

$$|\tilde{\Psi}_{k+1}(\iota)| \le \left|1 - \frac{\eta \Delta u_k^2(\iota)}{\mu + \Delta u_k^2(\iota)}\right||\tilde{\Psi}_k(\iota)| + \frac{\eta b_\xi}{2\sqrt{\mu}}. \tag{20}$$

From the selection of η and μ, it is not difficult to get

$$0 < \left|1 - \frac{\eta \Delta u_k^2(\iota)}{\mu + \Delta u_k^2(\iota)}\right| \le M_3 < 1 \tag{21}$$

where M_3 is unknown.

Taking (21) into (20) renders

$$\begin{aligned} |\tilde{\Psi}_{k+1}(\iota)| &\le M_3|\tilde{\Psi}_k(\iota)| + \Theta \\ &\vdots \\ &\le M_3^k|\tilde{\Psi}_1(\iota)| + \frac{\Theta\left(1 - M_3^k\right)}{1 - M_3} \end{aligned} \tag{22}$$

where $\Theta = (\eta b_\xi / 2\sqrt{\mu})$. Therefore, $\tilde{\Psi}_k(\iota)$ is bounded by $(\Theta / 1 - M_3)$ as $k \to \infty$.

With the boundedness of $\hat{\Psi}_k(\iota)$ established above, the boundedness of observation error is presented afterward.

Theorem 2: Choosing l_1, l_2, and l_3 satisfying $0 < l_1 < 1$, $0 < l_3 < 1$, and (6), the observation error system composed of (4) and (13) with the triggering scheme (9)–(16) is uniformly ultimately bounded under Assumptions 1–3.

Proof:

Case I: At the triggering moments, combining (4) and (13) yields

$$\tilde{g}_k(\iota + 1) = A\tilde{g}_k(\iota) + \begin{bmatrix} \tilde{\Psi}_k(\iota)[u_k(\iota) - u_k(\iota - 1)] \\ \xi_k(\iota + 1) - l_3\xi_k(\iota) \end{bmatrix} \tag{23}$$

where $\tilde{g}_k(\iota) = g_k(\iota) - \hat{g}_k(\iota)$, $\hat{g}_k(\iota) = [\hat{\tilde{g}}_k(\iota), \hat{\tilde{\xi}}_k(\iota)]^{\mathrm{T}}$, $A = \begin{bmatrix} 1 - l_1 & 1 \\ -l_2 & l_3 \end{bmatrix}$.

From the selection rule of l_1, l_2, and l_3, one has $S(A) = \bar{\theta} < 1$. According to Lemma 2, there exists ϵ such that

$$\|A\|_p \le S(A) + \epsilon \le M_4 < 1 \tag{24}$$

where $0 < M_4 < 1$.

Treating (2) with Lemma 1 and Theorem 1 produces

$$\left\| \begin{bmatrix} \tilde{\Psi}_k(\iota)[u_k(\iota) - u_k(\iota - 1)] \\ \xi_k(\iota + 1) - l_3\xi_k(\iota) \end{bmatrix} \right\|_p \le M_5 \tag{25}$$

where $M_5 = ((b_{\tilde{\Psi}} b_{\Delta u})^p + ((1 + l_3) b_\xi)^p)^{1/p}$ and $b_{\tilde{\Psi}}$ is the bound of $|\tilde{\Psi}_k(\iota)|$.

Combining (23)–(25) supplies

$$\begin{aligned} \|\tilde{g}_k(\iota + 1)\|_v &\le M_4\|\tilde{g}_k(\iota)\|_v + M_5 \\ &\vdots \\ &\le M_4^\iota\|\tilde{g}_k(1)\|_v + \frac{M_5\left(1 - M_4^\iota\right)}{1 - M_4} \end{aligned} \tag{26}$$

which means that $\tilde{g}_k(\iota)$ is bounded by $(M_5 / 1 - M_4)$ as $\iota \to \infty$.

Case II: During the consecutive triggering instants, substituting (12) into (13) renders

$$\tilde{q}_k(\iota + 1) = B\tilde{q}_k(\iota) + \begin{bmatrix} \tilde{\Psi}_k(\iota)[u_k(\iota) - u_k(\iota - 1)] \\ \xi_k(\iota + 1) - l_3\xi_k(\iota) \end{bmatrix} \tag{27}$$

where $\tilde{q}_k(\iota) = q_k(\iota) - \hat{q}_k(\iota)$, $q_k(\iota) = [\hat{y}_k(\iota), \xi_k(\iota)]^{\mathrm{T}}$, $\hat{q}_k(\iota) = [\hat{\tilde{g}}_k(\iota), \hat{\tilde{\xi}}_k(\iota)]^{\mathrm{T}}$, $B = \begin{bmatrix} 1 - l_1 & 0 \\ -l_2 & l_3 \end{bmatrix}$.

From the selection rule of l_1 and l_3, it gives $S(B) < 1$. Then, according to Lemma 2, there exists ϵ such that

$$\|B\|_p \le S(B) + \epsilon \le s_5 < 1 \tag{28}$$

where $0 < s_5 < 1$.

Integrating (25) and (28) into (27) yields

$$\begin{aligned} \|\tilde{q}_k(\iota + 1)\|_v &\le s_5\|\tilde{q}_k(\iota)\|_v + M_5 \\ &\vdots \\ &\le s_5^\iota\|\tilde{q}_k(1)\|_v + \frac{M_5\left(1 - s_5^\iota\right)}{1 - s_5}. \end{aligned} \tag{29}$$

Therefore, $\tilde{q}_k(\iota)$ is bounded by $(M_5 / 1 - s_5)$ as $\iota \to \infty$.

Remark 8: During the consecutive triggering instants, ESO in [30] leads to $S(B)_{\max} = 1$, which may not make the observation error converge. In this article, an extra l_3 meeting $0 < l_3 < 1$ is introduced to not only treat the output ET case but also reduce observation error boundary.

Based on Theorems 1 and 2, the boundedness proof of $e_k(\iota)$ is presented in the following theorem.

Theorem 3: If the system (1) meets Assumptions 1–3 and select ρ and λ meeting $0 < \rho < 1$ and $\lambda > 0$, the tracking errors $e_k(\iota)$ with the triggering scheme (9)–(16) is uniformly ultimately bounded.

Proof:

Case I: At the triggering iterations ($k = k_l$), substituting (11) into (3) gives

$$\begin{aligned} e_{k+1}(\iota + 1) &= y^*(\iota + 1) - y_{k+1}(\iota + 1) \\ &= \left(1 - \frac{\rho \Psi_{k+1}(\iota)\hat{\Psi}_{k+1}(\iota)}{\lambda + \hat{\Psi}_{k+1}^2(\iota)}\right)e_k(\iota + 1) \\ &\quad + \frac{\rho \Psi_{k+1}(\iota)\hat{\Psi}_{k+1}(\iota)\hat{\tilde{\xi}}_{k+1}(\iota)}{\lambda + \hat{\Psi}_{k+1}^2(\iota)} - \xi_{k+1}(\iota). \end{aligned} \tag{30}$$

Taking the absolute value operation to (30) yields

$$|e_{k+1}(\iota+1)| \le |\left(1-\frac{\rho\Psi_{k+1}(\iota)\hat{\Psi}_{k+1}(\iota)}{\lambda+\hat{\Psi}^2_{k+1}(\iota)}\right)||e_k(\iota+1)| + |\frac{\rho\Psi_{k+1}(\iota)\hat{\Psi}_{k+1}(\iota)}{\lambda+\hat{\Psi}^2_{k+1}(\iota)}|b_{\hat{g}}+b_{\xi} \tag{31}$$

where $b_{\hat{g}}$ is the bound of $|\hat{\bar{g}}_{k+1}(\iota)|$.

With the help of (10) and $2\mathbb{A}\mathbb{B} \le \mathbb{A}^2+\mathbb{B}^2$, one has

$$0 < \frac{\rho\Psi_{k+1}(\iota)\hat{\Psi}_{k+1}(\iota)}{\lambda+\hat{\Psi}^2_{k+1}(\iota)} < \frac{\rho|\Psi_{k+1}(\iota)||\hat{\Psi}_{k+1}(\iota)|}{2\sqrt{\lambda}|\hat{\Psi}_{k+1}(\iota)|} = \frac{\rho|\Psi_{k+1}(\iota)|}{2\sqrt{\lambda}}. \tag{32}$$

From the selection rule of ρ and λ, it gets

$$\frac{\rho|\Psi_{k+1}(\iota)|}{2\sqrt{\lambda}} \le \frac{\rho b}{2\sqrt{\lambda}} < 1. \tag{33}$$

Combining (32) and (33) supplies

$$0 < |1-\frac{\rho\Psi_{k+1}(\iota)\hat{\Psi}_{k+1}(\iota)}{\lambda+\hat{\Psi}^2_{k+1}(\iota)}| \le M_6 < 1 \tag{34}$$

where M_6 is unknown.

Taking (32)–(34) into (31) provides

$$\begin{aligned}|e_{k+1}(\iota+1)| &\le M_6|e_k(\iota+1)| + b_{\hat{g}} + b_{\xi}\\ &\vdots\\ &\le M_6^k|e_1(\iota+1)| + \frac{\left(b_{\hat{g}}+b_{\xi}\right)\left(1-M_6^k\right)}{1-M_6}.\end{aligned} \tag{35}$$

Therefore, $e_k(\iota)$ is bounded by $((b_{\hat{g}}+b_{\xi})/[1-M_6])$ as $k \to \infty$.

Case II: During the interevent iterations ($k_l < k < k_{l+1}$), (14) gives $\hat{e}_k(\iota+1) = e_k(\iota+1) + e_{ETk}(\iota+1)$. Then, combining (11) and (3) yields

$$\begin{aligned}e_{k+1}(\iota+1) &= y^*(\iota+1) - y_{k+1}(\iota+1)\\ &= \left(1-\frac{\rho\Psi_{k+1}(\iota)\hat{\Psi}_{k+1}(\iota)}{\lambda+\hat{\Psi}^2_{k+1}(\iota)}\right)e_k(\iota+1)\\ &\quad - \frac{\rho\Psi_{k+1}(\iota)\hat{\Psi}_{k+1}(\iota)}{\lambda+\hat{\Psi}^2_{k+1}(\iota)}e_{ETk}(\iota+1)\\ &\quad + \frac{\rho\Psi_{k+1}(\iota)\hat{\Psi}_{k+1}(\iota)}{\lambda+\hat{\Psi}^2_{k+1}(\iota)}\hat{\bar{g}}_{k+1}(\iota) - \xi_{k+1}(\iota).\end{aligned} \tag{36}$$

Recalling Theorems 1 and 2, one has $\upsilon = \rho\hat{\Psi}^2_{k+1}(\iota)/(\lambda+\hat{\Psi}^2_{k+1}(\iota))$ and $\xi_{k+1}(\iota) = \hat{\bar{g}}_{k+1}(\iota)$. Then, applying these replacements to (36) gets

$$\begin{aligned}e_{k+1}(\iota+1) &= (1-\upsilon)e_k(\iota+1) - \upsilon e_{ETk}(\iota+1)\\ &\quad - (1-\upsilon)\hat{\bar{g}}_{k+1}(\iota).\end{aligned} \tag{37}$$

Choose the candidate Lyapunov function $V_k = e_k^2(\iota+1)$ and take its difference operation provides

$$\Delta V_{k+1}(\iota+1) = e^2_{k+1}(\iota+1) - e^2_k(\iota+1). \tag{38}$$

Integrating (37) into (38) yields

$$\begin{aligned}\Delta V_{k+1}(\iota+1) &= \Big[(1-\upsilon)e_k(\iota+1) - \upsilon e_{ETk}(\iota+1)\\ &\quad -(1-\upsilon)\hat{\bar{g}}_{k+1}(\iota)\Big]^2 - e_k^2(\iota+1).\end{aligned} \tag{39}$$

Combining (15) and (39) renders $\Delta V_{k+1}(\iota+1) \le 0$.

Unifying the above two cases, $e_k^2(\iota)$ is uniformly ultimately bounded.

Remark 9: Due to disturbances, $e_k(\iota)$ converges to $[(b_{\hat{g}}+b_{\xi})/1-M_6]$ determined by ρ and λ. Therefore, properly choosing them could make $[(b_{\hat{g}}+b_{\xi})/1-M_6]$ be small enough.

B. MIMO System

The following assumption and lemma are necessary for the derivation.

Assumption 4 [16]: The signs of the all elements of matrix $\Phi_k(\iota) \in \mathcal{R}^{m\times m}$ are unchanged. Without loss generality, it is assumed that $\psi_{pjk}(\iota) > 0$ and $\psi_{ppk}(\iota) > 0$, $p, j \in [1, m]$, where $\psi_{pjk}(\iota)$ and $\psi_{ppk}(\iota)$ are the elements of $\Phi_k(\iota)$.

Lemma 3 [35]: Given the system

$$\bar{E}_{k+1}(\iota+1) = \bar{\Pi}_k(\iota)\bar{E}_k(\iota+1) + \bar{\Gamma}_k(\iota) \tag{40}$$

where $\bar{E}_k(\iota+1) \in \mathcal{R}^m$ denotes the state, $\bar{\Gamma}_k(\iota) \in \mathcal{R}^m$ is the input, and $\bar{\Pi}_k(\iota) \in \mathcal{R}^{m\times m}$ is a bounded mapping matrix, i.e., $\|\bar{\Pi}_k(\iota)\| \le \alpha_{\bar{\Pi}}$ with $\alpha_{\bar{\Pi}} > 0$. If for any given integer $\iota \in \{0, 1, \ldots\}$, there exists some iteration sequence $\{\zeta_s(\iota): s \in \mathrm{Z}_+\}$, where $\{\zeta_0(\iota) = 0\}$ and $0 < \zeta_{s+1}(\iota) - \zeta_s(\iota) \le \delta(\iota)$ for some finite positive integer $1 \le \delta(\iota) < \infty$, such that

$$\left\|P_{j=\zeta_s(\iota)}^{\zeta_{s+1}(\iota)}\bar{\Pi}_j(\iota)\right\| \le \varrho < 1$$

for all $s \in \mathrm{Z}_+$. Then for any initial $\bar{E}_{k0}(\iota)$ ($k_0 \in \mathrm{Z}_+$) and any bounded $\bar{\Gamma}_k(\iota)$, the solution to (40) exists for all $k \ge k_0$ and satisfies

$$\begin{aligned}\|\bar{E}_k(\iota)\| &\le \varrho^{\bar{s}_k(\iota)-s_{k_0}(\iota)}\alpha_{\bar{\Pi}}^{2(\delta(\iota)-1)}\|\bar{E}_{k_0}(\iota)\|\\ &\quad + \Bigg(\varrho^{\bar{s}_k(\iota)-s_{k_0}(\iota)}\alpha_{\bar{\Pi}}^{\delta(\iota)-1}\frac{1-\alpha_{\bar{\Pi}}^{\delta(\iota)-1}}{1-\alpha_{\bar{\Pi}}}\\ &\quad + \frac{1-\varrho^{\bar{s}_k(\iota)-s_{k_0}(\iota)}}{1-\varrho}\alpha_{\bar{\Pi}}^{\delta(\iota)-1}\frac{1-\alpha_{\bar{\Pi}}^{\delta(\iota)}}{1-\alpha_{\bar{\Pi}}} + \frac{1-\alpha_{\bar{\Pi}}^{\delta(\iota)-1}}{1-\alpha_{\bar{\Pi}}}\Bigg)\\ &\quad \times \max_{k_0\le i\le k-1}\|\bar{\Gamma}_i(\iota)\|\end{aligned}$$

where, for every $k \in \mathrm{Z}_+$, $\bar{s}_k(\iota) \in \mathrm{Z}_+$, and $s_k(\iota) \in \mathrm{Z}_+$ denote the greatest and least integers such that $\zeta_{\bar{s}_k(\iota)}(\iota) \le k < \zeta_{\bar{s}_k(\iota)+1}(\iota)$ and $\zeta_{s_k(\iota)-1}(\iota) \le k < \zeta_{s_k(\iota)}(\iota)$ hold, respectively.

Similar to SISO, (9)–(16) are extended for MIMO case as

$$\hat{\Phi}_{k+1}(\iota) = \begin{cases}\hat{\Phi}_k(\iota) + \dfrac{\eta K_k(\iota)\Delta U_k^{\mathrm{T}}(\iota)}{\mu+\|\Delta U_k(\iota)\|^2}, & k = k_l\\ \hat{\Phi}_k(\iota), & k_l < k < k_{l+1}\end{cases} \tag{41}$$

$$\begin{aligned}&\hat{\psi}_{ppk}(\iota) = \hat{\psi}_{pp1}(1)\\ &\text{if } |\hat{\psi}_{ppk}(\iota)| < \omega \text{ or } \operatorname{sign}\left(\hat{\psi}_{ppk}(\iota)\right) \ne \operatorname{sign}\left(\hat{\psi}_{pp1}(1)\right)\\ &\hat{\psi}_{pjk}(\iota) = \hat{\psi}_{pj1}(1), \text{ if } sign\left(\hat{\psi}_{pjk}(\iota)\right) \ne \operatorname{sign}\left(\hat{\psi}_{pj1}(1)\right)\end{aligned} \tag{42}$$

$$\begin{cases} U_{k+1}(\iota) = U_k(\iota) + \dfrac{\rho\hat{\Phi}_{k+1}^{\mathrm{T}}(\iota)\left[E_k(\iota+1) - \hat{\bar{G}}_{k+1}(\iota)\right]}{\lambda + \|\hat{\Phi}_{k+1}(\iota)\|^2}, k = k_l \\ U_{k+1}(\iota) = U_k(\iota) + \dfrac{\rho\hat{\Phi}_{k+1}^{\mathrm{T}}(\iota)\left[\hat{E}_k(\iota+1) - \hat{\bar{G}}_{k+1}(\iota)\right]}{\lambda + \|\hat{\Phi}_{k+1}(\iota)\|^2} \\ \qquad k_l < k < k_{l+1} \end{cases} \tag{43}$$

$$\begin{cases} \begin{cases} \hat{\bar{G}}_k(\iota+1) = \hat{\bar{G}}_k(\iota) + \hat{\bar{\bar{G}}}_k(\iota) + \hat{\Phi}_k(\iota)(U_k(\iota) - U_k(\iota-1)) \\ \quad + l_1\left(Y_k(\iota) - \hat{\bar{G}}_k(\iota)\right) \\ \hat{\bar{\bar{G}}}_k(\iota+1) = l_3\hat{\bar{\bar{G}}}_k(\iota) + l_2\left(Y_k(\iota) - \hat{\bar{G}}_k(\iota)\right) \end{cases} , k = k_l \\ \begin{cases} \hat{\bar{G}}_k(\iota+1) = \hat{\bar{G}}_k(\iota) + \hat{\bar{\bar{G}}}_k(\iota) + \hat{\Phi}_k(\iota)(U_k(\iota) - U_k(\iota-1)) \\ \qquad + l_1\left(\hat{Y}_k(\iota) - \hat{\bar{G}}_k(\iota)\right) \\ \hat{\bar{\bar{G}}}_k(\iota+1) = l_3\hat{\bar{\bar{G}}}_k(\iota) + l_2\left(\hat{Y}_k(\iota) - \hat{\bar{G}}_k(\iota)\right) \end{cases} \\ \qquad k_l < k < k_{l+1} \end{cases} \tag{44}$$

where $K_k(\iota) = \Delta Y_k(\iota+1) - \hat{\Phi}_k(\iota)\Delta U_k(\iota)$, $E_k(\iota) = Y^*(\iota) - Y_k(\iota)$, and $\hat{E}_k(\iota) = Y^*(\iota) - \hat{Y}_k(\iota)$. $Y_k(\iota) \in \mathcal{R}^m$, $Y^*(\iota) \in \mathcal{R}^m$, and $U_k(\iota) \in \mathcal{R}^m$ are output, desired output and input, respectively. $\hat{Y}_k(\iota)$ means the estimated $Y_k(\iota)$. $\hat{\Phi}_k(\iota) \in \mathcal{R}^{m\times m}$, $\hat{\bar{G}}_k(\iota) \in \mathcal{R}^m$, and $\hat{\bar{\bar{G}}}_k(\iota) \in \mathcal{R}^m$ denote the estimated PPD, output, and uncertainties, respectively. Moreover, $0 < \eta < 2$, $\mu > 0$, $\rho > 0$, and $\lambda > 0$.

Now it is the position to put forward the event-triggering condition for this case as

$$D\Big(R(\cdot)\Big) > E_k(\iota+1)^{\mathrm{T}}E_k(\iota+1) \tag{45}$$

where $R(\cdot) = ((I-Q)\ E_k(\iota+1) - QE_{ETk}(\iota+1) - (I-Q)\hat{\bar{\bar{G}}}_{k+1}(\iota))^{\mathrm{T}}((I-Q)\ E_k(\iota+1) - QE_{ETk}(\iota+1) - (I-Q)\hat{\bar{\bar{G}}}_{k+1}(\iota))$, $Q = \rho\hat{\Phi}_{k+1}(\iota)\hat{\Phi}_{k+1}^{\mathrm{T}}(\iota)/(\lambda + \|\hat{\Phi}_{k+1}(\iota)\|^2)$, $E_{ETk}(\iota) = Y_k(\iota) - \hat{Y}_k(\iota)$ and $D(R(\cdot))$ is a dead-zone operator as follows:

$$D\Big(R(\cdot)\Big) = \begin{cases} R(\cdot), & \text{if } \|E_k(\iota+1)\| > H_e \\ 0, & \text{otherwise} \end{cases}$$

where I denotes the unit matrix with appropriate dimensions.

On the basis of (41)–(45), the boundedness of $\hat{\Phi}_k(\iota)$ for MIMO case is proposed as below.

Theorem 4: If the system (1) meets Assumptions 1–4 and select η and μ meeting $0 < \eta < 2$ and $\mu > 0$, $\hat{\Phi}_k(\iota)$ estimated by (41) under (45) is ultimately uniformly bounded.

Proof: Similar to SISO, only consider the triggered $\hat{\Phi}_k(\iota)$.

Let $\hat{\Phi}_k(\iota) = \left[\hat{\bar{\psi}}_{1k}^{\mathrm{T}}(\iota), \hat{\bar{\psi}}_{2k}^{\mathrm{T}}(\iota), \ldots, \hat{\bar{\psi}}_{mk}^{\mathrm{T}}(\iota)\right]^{\mathrm{T}}$, $\hat{\bar{\psi}}_{jk}(\iota) = \left[\hat{\phi}_{j1k}(\iota), \hat{\phi}_{j2k}(\iota), \ldots, \hat{\phi}_{jmk}(\iota)\right]$, $j = 1, 2, \ldots, m$. Then, (41) is converted to

$$\hat{\bar{\psi}}_{jk+1}(\iota) = \hat{\bar{\psi}}_{jk}(\iota) + \frac{\eta\chi_{jk}(\iota)\Delta U_k(\iota)^{\top}}{\mu + \|\Delta U_k(\iota)\|^2} \tag{46}$$

where $\chi_{jk}(\iota) = \Delta Y_{jk}(\iota+1) - \hat{\bar{\psi}}_{jk}(\iota)\Delta U_k(\iota)$.

Deducting $\bar{\bar{\psi}}_{jk}(\iota)$ on both sides of (46) renders

$$\tilde{\bar{\psi}}_{jk+1}(\iota) = \tilde{\bar{\psi}}_{jk}(\iota) - \frac{\eta\tilde{\bar{\psi}}_{jk}(\iota)\Delta U_k(\iota)\Delta U_k^{\top}(\iota)}{\mu + \|\Delta U_k(\iota)\|^2} + \frac{\eta\Xi_k(\iota)\Delta U_k^{\top}(\iota)}{\mu + \|\Delta U_k(\iota)\|^2} + \bar{\bar{\psi}}_{jk}(\iota) - \bar{\bar{\psi}}_{jk+1}(\iota) \tag{47}$$

where $\tilde{\bar{\psi}}_{jk}(\iota) = \hat{\bar{\psi}}_{jk}(\iota) - \bar{\bar{\psi}}_{jk}(\iota)$ and $\Xi_k(\iota) \in \mathcal{R}^m$ denotes uncertainties.

Defining

$$\Lambda_k(\iota) = \left\| \tilde{\bar{\psi}}_{jk}(\iota) - \frac{\eta\tilde{\bar{\psi}}_{jk}(\iota)\Delta U_k(\iota)\Delta U_k^{\top}(\iota)}{\mu + \|\Delta U_k(\iota)\|^2} \right\|$$

gives

$$\Lambda_k(\iota)^2 = \|\tilde{\bar{\psi}}_{jk}(\iota)\|^2 + \left(-2 + \frac{\eta\|\Delta U_k(\iota)\|^2}{\mu + \|\Delta U_k(\iota)\|^2} \right) \times \frac{\eta\|\tilde{\bar{\psi}}_{jk}(\iota)\Delta U_k(\iota)\|^2}{\mu + \|\Delta U_k(\iota)\|^2}. \tag{48}$$

From the selection rule of η and μ, one has

$$\left(-2 + \frac{\eta\|\Delta U_k(\iota)\|^2}{\mu + \|\Delta U_k(\iota)\|^2} \right) < 0. \tag{49}$$

Substituting (49) into (48) provides

$$\Lambda_k(\iota) \le d_1\|\tilde{\bar{\psi}}_{jk}(\iota)\| \tag{50}$$

where $0 < d_1 < 1$.

With the help of $2\mathbb{A}\mathbb{B} \le \mathbb{A}^2 + \mathbb{B}^2$, one gets

$$\left\| \frac{\eta\Xi_k(\iota)\Delta U_k^{\mathrm{T}}(\iota)}{\mu + \|\Delta U_k(\iota)\|^2} \right\| \le \frac{\eta b_{\Xi}}{2\sqrt{\mu}} \tag{51}$$

where b_{Ξ} is the bound of $\|\Xi_k(\iota)\|$.

Resorting to Remark 2, (47) is rewritten as

$$\tilde{\bar{\psi}}_{jk+1}(\iota) = \tilde{\bar{\psi}}_{jk}(\iota) - \frac{\eta\tilde{\bar{\psi}}_{jk}(\iota)\Delta U_k(\iota)\Delta U_k^{\top}(\iota)}{\mu + \|\Delta U_k(\iota)\|^2} + \frac{\eta\Xi_k(\iota)\Delta U_k^{\top}(\iota)}{\mu + \|\Delta U_k(\iota)\|^2}. \tag{52}$$

Integrating (50) and (51) into (52) yields

$$\begin{aligned} \|\tilde{\bar{\psi}}_{jk+1}(\iota)\| &\le d_1\|\tilde{\bar{\psi}}_{jk}(\iota)\| + \sigma \\ &\vdots \\ &\le d_1^k\|\tilde{\bar{\psi}}_{j1}(\iota)\| + \frac{\sigma\left(1 - d_1^k\right)}{1 - d_1} \end{aligned}$$

where $\sigma = (\eta b_{\Xi}/2\sqrt{\mu})$. Therefore, $\tilde{\bar{\psi}}_{jk}(\iota)$ is bounded by $(\sigma/1 - d_1)$ as $k \to \infty$, so does the $\hat{\Phi}_k(\iota)$.

Based on Theorem 4, Theorem 5 extended from Theorem 2 is proposed as below. ■

Theorem 5: Choosing l_1, l_2, and l_3 satisfying $0 < l_1 < 1$, $0 < l_3 < 1$, and (6), the observation error system composed of (4) and (44) with the triggering scheme (41)–(45) is uniformly ultimately bounded under Assumptions 1–4.

Case I: At triggering moments, (44) gives

$$\tilde{G}_k(\iota+1) = A\tilde{G}_k(\iota) + \begin{bmatrix} \tilde{\Phi}_k(\iota)[U_k(\iota) - U_k(\iota-1)] \\ \Xi_k(\iota+1) - l_3\Xi_k(\iota) \end{bmatrix} \quad (53)$$

where $\tilde{G}_k(\iota) = G_k(\iota) - \hat{G}_k(\iota)$, $\hat{G}_k(\iota) = [\hat{\bar{G}}_k(\iota), \hat{\bar{\bar{G}}}_k(\iota)]^{\mathrm{T}}$, $G_k(\iota) = [Y_k(\iota), \Xi_k(\iota)]^{\mathrm{T}}$ and $A = \begin{bmatrix} 1-l_1 & 1 \\ -l_2 & l_3 \end{bmatrix}$.

From the selection rule of l_1, l_2, and l_3, it gives $S(A) = \bar{\theta} < 1$. As a result, adopting Lemma 2 provides

$$\|A\|_p \le S(A) + \epsilon \le d_3 < 1 \quad (54)$$

where $0 < d_3 < 1$.

Applying (2) with Lemma 1 and Theorem 4 yields

$$\left\| \begin{bmatrix} \tilde{\Phi}_k(\iota)[U_k(\iota) - U_k(\iota-1)] \\ \Xi_k(\iota+1) - l_3\Xi_k(\iota) \end{bmatrix} \right\|_p \le d_4 \quad (55)$$

where $d_4 = ((b_{\tilde{\Phi}} b_{\Delta u})^p + ((1+l_3) b_{\Xi})^p)^{1/p}$ and $b_{\tilde{\Phi}}$ is the bound of $\|\tilde{\Phi}_k(\iota)\|$.

Combining (53)–(55) supplies

$$\begin{aligned} \|\tilde{G}_k(\iota+1)\|_v &\le d_3\|\tilde{G}_k(\iota)\|_v + d_4 \\ &\vdots \\ &\le d_3^{\iota}\|\tilde{G}_k(1)\|_v + \frac{d_4(1-d_3^{\iota})}{1-d_3}. \end{aligned}$$

Therefore, $\tilde{G}_k(\iota)$ is bounded by $(d_4/1-d_3)$ as $\iota \to \infty$.

Case II: During two consecutive triggering instants, taking (12) to (44) renders

$$\tilde{\bar{q}}_k(\iota+1) = B\tilde{\bar{q}}_k(\iota) + \begin{bmatrix} \tilde{\Phi}_k(\iota)[U_k(\iota) - U_k(\iota-1)] \\ \Xi_k(\iota+1) - l_3\Xi_k(\iota) \end{bmatrix} \quad (56)$$

where $\tilde{\bar{q}}_k(\iota) = \bar{q}_k(\iota) - \hat{\bar{q}}_k(\iota)$, $\bar{q}_k(\iota) = [\hat{Y}_k(\iota), \Xi_k(\iota)]^{\mathrm{T}}$, $\hat{\bar{q}}_k(\iota) = [\hat{\bar{G}}_k(\iota), \hat{\bar{\bar{G}}}_k(\iota)]^{\mathrm{T}}$, $B = \begin{bmatrix} 1-l_1 & 0 \\ -l_2 & l_3 \end{bmatrix}$.

According to the selection rule of l_1 and l_3, one gets $S(B) < 1$. Consequently, utilizing Lemma 2 provides

$$\|B\|_p \le S(B) + \epsilon \le s_6 < 1 \quad (57)$$

where $0 < s_6 < 1$.

Integrating (55) and (57) into (56) yields

$$\begin{aligned} \|\tilde{\bar{q}}_k(\iota+1)\|_v &\le s_6\|\tilde{\bar{q}}_k(\iota)\|_v + d_4 \\ &\vdots \\ &\le s_6^{\iota}\|\tilde{\bar{q}}_k(1)\|_v + \frac{d_4(1-s_6^{\iota})}{1-s_6}. \end{aligned} \quad (58)$$

Therefore, $\tilde{G}_k(\iota)$ is bounded by $(d_4/1-s_6)$ as $\iota \to \infty$.

The boundedness proof of $E_k(\iota)$ applying ETMFILC scheme for MIMO system is supplied in Theorem 6.

Theorem 6: If the system (1) meets Assumptions 1–4 and select ρ and λ meeting $0 < \rho < 1$ and $\lambda > 0$, the tracking errors $E_k(\iota)$ with the triggering scheme (41)–(45) is ultimately uniformly bounded.

Proof:

Case I: At the triggering iterations ($k = k_l$), substituting (43) to (3) supplies

$$\begin{aligned} E_{k+1}(\iota+1) &= Y^*(\iota+1) - Y_{k+1}(\iota+1) \\ &= \Pi_k(\iota)E_k(\iota+1) + \Gamma_k(\iota) \end{aligned} \quad (59)$$

where

$$\Pi_k(\iota) = I - \frac{\rho\Phi_{k+1}(\iota)\hat{\Phi}_{k+1}^{\mathrm{T}}(\iota)}{\lambda + \|\hat{\Phi}_{k+1}(\iota)\|^2}$$

and

$$\Gamma_k(\iota) = \frac{\rho\Phi_{k+1}(\iota)\hat{\Phi}_{k+1}^{\mathrm{T}}(\iota)\hat{\bar{\bar{G}}}_{k+1}(\iota)}{\lambda + \|\hat{\Phi}_{k+1}(\iota)\|^2} - \Xi_{k+1}(\iota).$$

The positive-definiteness of $\Phi_{k+1}(\iota)\hat{\Phi}_{k+1}^{\mathrm{T}}(\iota)$ is provided by Assumption 4 and (42). Moreover, $\Phi_{k+1}(\iota)$ and $\hat{\Phi}_{k+1}(\iota)$ are bounded. As a result, from the selection rule of ρ and λ, there exists a positive constant d_6 such that

$$\|\Pi_k(\iota)\| = \|I - \frac{\rho\Phi_{k+1}(\iota)\hat{\Phi}_{k+1}^{\mathrm{T}}(\iota)}{\lambda + \|\hat{\Phi}_{k+1}(\iota)\|^2}\| \le d_6 < 1 \quad (60)$$

which yields

$$\left\| P_{j=1}^{k}\Pi_j(\iota) \right\| \le P_{j=1}^{k}\left\| \Pi_j(\iota) \right\| \le d_6^k < 1$$

and

$$\|\Gamma_k(\iota)\| \le b_{\hat{G}} + b_{\Xi}$$

where $b_{\hat{G}}$ is the bound of $\|\hat{\bar{\bar{G}}}_k(\iota+1)\|$.

Applying Lemma 3 to (59) for $\alpha_\Pi < 1$, $\varrho = \alpha_\Pi$, $\delta(\iota) = 1$, $\bar{s}_k(\iota) = k$ and $s_{k_0}(\iota) = 1$ renders

$$\|E_{k+1}(\iota)\| \le d_6^{k-1}\|E_1(\iota)\| + \frac{1-d_6^{k-1}}{1-d_6}\max_{k_0 \le i \le k-1}\|\Gamma_i(\iota)\| \quad (61)$$

Therefore, $E_k(\iota)$ is bounded by $(b_{\hat{G}} + b_{\Xi}/1-d_6)$ as $k \to \infty$.

Case II: During the interevent iterations ($k_l < k < k_{l+1}$), taking (43) into (3) gets

$$\begin{aligned} E_{k+1}(\iota+1) = E_k(\iota+1) - \Xi_{k+1}(\iota) \\ - \frac{\rho\Phi_{k+1}(\iota)\hat{\Phi}_{k+1}^{\mathrm{T}}(\iota)}{\lambda + \|\hat{\Phi}_{k+1}(\iota)\|^2}\left(\hat{E}_k(\iota+1) - \hat{\bar{\bar{G}}}_{k+1}(\iota)\right). \end{aligned} \quad (62)$$

Resorting to Remark 2, $\Psi_{k+1}(\iota)$ is replaced by $\hat{\Phi}_{k+1}(\iota)$. Similarly, $\hat{\bar{\bar{G}}}_{k+1}(\iota) = \Xi_{k+1}(\iota)$. Utilizing these replacements to (62) produces

$$\begin{aligned} E_{k+1}(\iota+1) = (I-Q)E_k(\iota+1) - QE_{ETk}(\iota+1) \\ - (I-Q)\hat{\bar{\bar{G}}}_{k+1}(\iota). \end{aligned} \quad (63)$$

Select the candidate Lyapunov function $V_{k+1}(\iota+1) = E_{k+1}(\iota+1)^{\mathrm{T}}E_{k+1}(\iota+1)$ and take its difference operation provides

$$\begin{aligned} &\Delta V_{k+1}(\iota+1) \\ &= E_{k+1}(\iota+1)^{\mathrm{T}}E_{k+1}(\iota+1) - E_k(\iota+1)^{\mathrm{T}}E_k(\iota+1). \end{aligned} \quad (64)$$

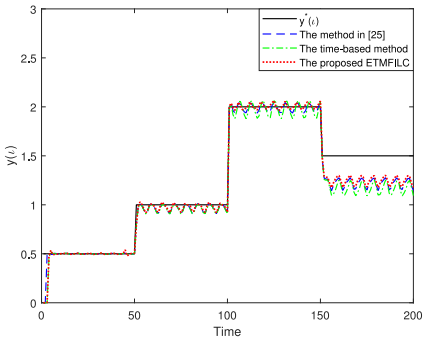

Fig. 2. $y(\iota)$ under three schemes for the 10th iteration.

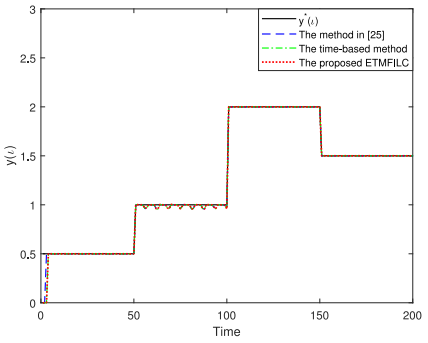

Fig. 3. $y(\iota)$ under three schemes for the 40th iteration.

Integrating (63) into (64) yields

$$\begin{aligned}\Delta V_{k+1}(\iota+1) = &\Big((I-Q)E_k(\iota+1) - QE_{ETk}(\iota+1) \\ &- (I-Q)\hat{\bar{G}}_{k+1}(\iota)\Big)^{\mathrm{T}}\Big((I-Q)E_k \\ &- QE_{ETk}(\iota+1) - (I-Q)\hat{\bar{G}}_{k+1}(\iota)\Big) \\ &- E_k(\iota+1)^{\mathrm{T}}E_k(\iota+1). \end{aligned} \tag{65}$$

Combining (45) and (65), $\Delta V_{k+1}(\iota+1) \leq 0$ holds.

Summarizing the above two cases, $E_k(\iota)$ is uniformly ultimately bounded.

IV. Numerical Example

In this part, two examples are supplied to verify the proposed ETMFILC schemes.

Example 1 (SISO): A steam-water heat exchanger system in [27] is

$$\begin{aligned} x(\iota) &= 1.5u(\iota) - 1.5u(\iota)^2 + 0.5u(\iota)^3 \\ y(\iota+1) &= 0.6y(\iota) - 0.1y(\iota-1) \\ &\quad + 1.2x(\iota) - 0.1x(\iota-1) + d(\iota) \end{aligned}$$

where $d(\iota) = 0.01\sin(t)$ is disturbance.

The expected trajectory is given as

$$y^*(\iota) = \begin{cases} 0.5, & 0 < \iota \leq 50 \\ 1, & 51 < \iota \leq 100 \\ 2, & 101 < \iota \leq 150 \\ 1, & 151 < \iota \leq 200. \end{cases}$$

Set $u_1(\iota) = 0$, $\hat{\bar{g}}_1(\iota) = 0$, $\hat{\Psi}_1(1) = 1.5$, $\hat{\Psi}_2(1) = 1.5$, $y_1(1)$=0. Moreover, the controller parameters are selected as $\eta = 0.01, \mu = 1, \rho = 0.6, \lambda = 0.6, H_e = 0.005, \omega = 10^{-4}$, $l_1 = 0.1$, $l_2 = 0.01$, $l_3 = 0.1$.

The outputs at the 10th, 40th, and 100th iterations with the proposed ETMFILC scheme, the one in [25] and the time-based method are given in Figs. 2–4, respectively. Fig. 5 describes the estimated uncertainties. The error curves with three schemes are provided in Fig. 6. Fig. 7 shows the triggering number per iteration. Figs. 8–10 show the release events at three specified instants. The comparison of transmission times is supplied in Table I.

From Figs. 2–4, it is seen that the more the iteration numbers is, the better the performance is. Fig. 5 indicates

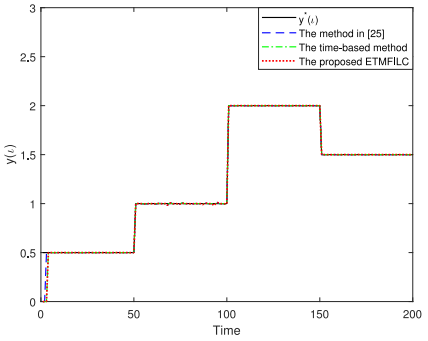

Fig. 4. $y(\iota)$ under three schemes for the 100th iteration.

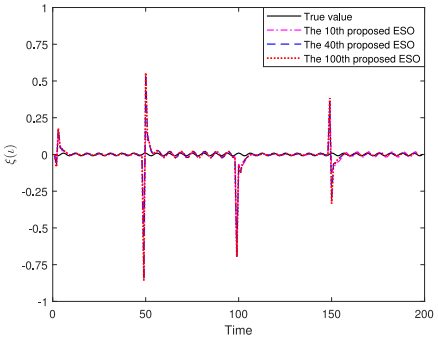

Fig. 5. Estimated $\xi(\iota)$ for different iterations.

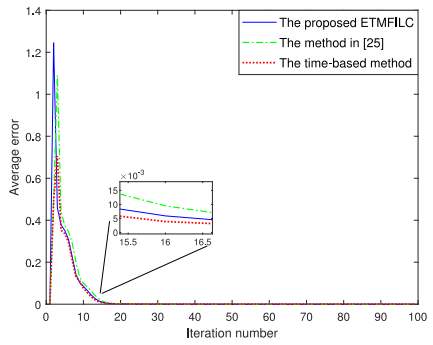

Fig. 6. Average errors with three schemes.

that the proposed ESO works well to estimate uncertainties. Figs. 7 and 10 indicate the effectiveness of the proposed triggering rule, which is further demonstrated by the comparison in Table I.

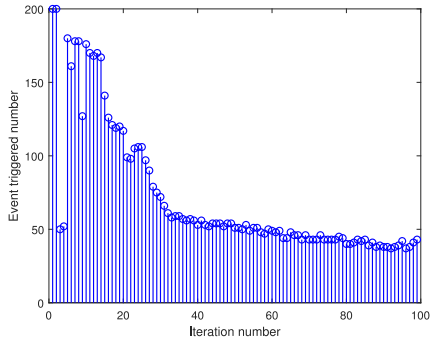

Fig. 7. Triggering number per iteration.

TABLE I
COMPARISON OF TRANSMITTED TIMES FOR 100 ITERATIONS

	The proposed ETMFILC	The method in [25]
Transmission times	7109	7836

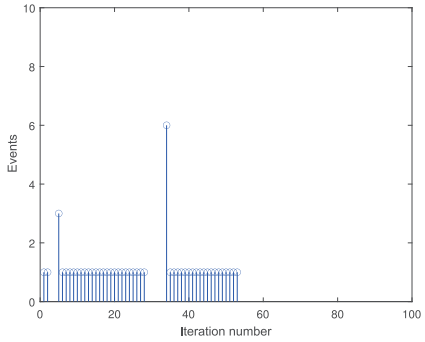

Fig. 8. Release events at $\iota = 55$.

Example 2 (MIMO): Consider the following three-tank system in [16] as:

$$\begin{cases} S_A \dfrac{dy_1(\iota)}{d\iota} = u_1(\iota) - Q_1(\iota) + d_1(\iota) \\ S_A \dfrac{dh(\iota)}{d\iota} = Q_1(\iota) - Q_2(\iota) \\ S_A \dfrac{dy_2(\iota)}{d\iota} = u_2(\iota) + Q_2(\iota) - Q_3(\iota) + d_2(\iota) \\ Q_1(\iota) = \alpha_1 z_1 S_n \mathrm{sgn}(y_1(\iota) - h(\iota))\sqrt{2g|y_1(\iota) - h(\iota)|} \\ Q_2(\iota) = \alpha_3 z_3 S_n \mathrm{sgn}(y_2(\iota) - h(\iota))\sqrt{2g|y_2(\iota) - h(\iota)|} \\ Q_3(\iota) = \alpha_2 z_2 S_n \mathrm{sgn}(h(\iota))\sqrt{2gh(\iota)} \end{cases}$$

where $d_1(\iota) = 0.1\sin(\iota/5)$ and $d_2(\iota) = 0.1\cos(\iota/5)$ are disturbances.

The expected trajectory to be tracked is designed as follows:

$$\begin{cases} y_1^*(\iota) = \sin(\pi\iota/200) + 0.4\cos(\pi\iota/80) \\ y_2^*(\iota) = 0.4\sin(\pi\iota/180) + \cos(\pi\iota/200). \end{cases}$$

Set $\rho = 0.88, \lambda = 0.01, \eta = 1, \mu = 0.01, H_e = 0.1, \omega = 10^{-4}, l_1 = 0.1, l_2 = 0.01, l_3 = 0.1, S_A = 0.0154, S_n = 5 * 10^{-5}, \alpha_1 z_1 = \alpha_2 z_2 = \alpha_3 z_3 = 0.3, g = 9.8, \Phi_1(1) = \Phi_1(2) = [1.5, 0.01; 0.01, 1.5], y_1(1) = y_1(2) = [2; 0], h_1(1) = h_1(2) = 0, u_1(1) = u_1(2) = [0; 0], \hat{\bar{\bar{g}}}_1(1) = \hat{\bar{g}}_1(1) = [0; 0]$.

The outputs y_1 and y_2 of the 5th, 15th, 50th iterations are given in Figs. 11–16 under three schemes. Figs. 17 and 18 display the estimated uncertainties. The average error curves under these schemes are shown in Figs. 19 and 20, respectively. The triggering number per iteration is provided in Fig. 21. Figs. 22–24 individually show the release events at

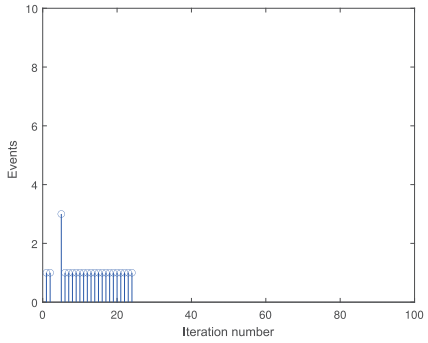

Fig. 9. Release events at $\iota = 75$.

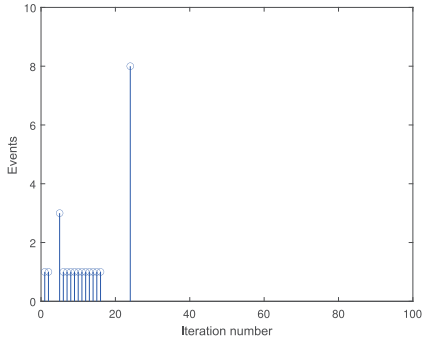

Fig. 10. Release events at $\iota = 95$.

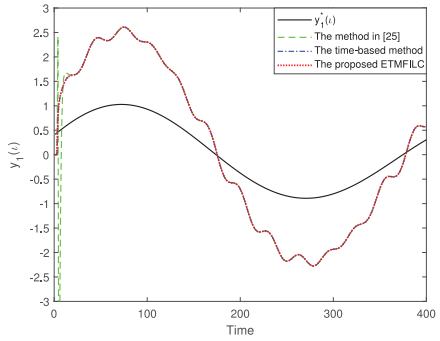

Fig. 11. $y_1(\iota)$ under three schemes for the 5th iteration.

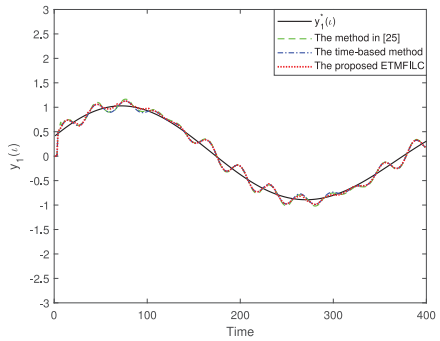

Fig. 12. $y_1(\iota)$ under three schemes for the 15th iteration.

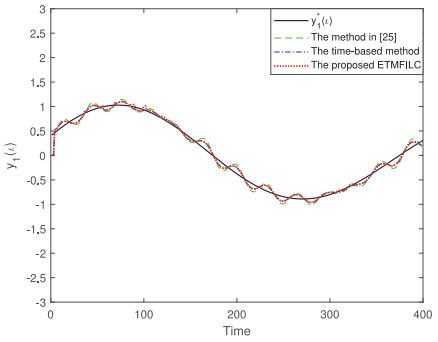

Fig. 13. $y_1(\iota)$ under three schemes for the 50th iteration.

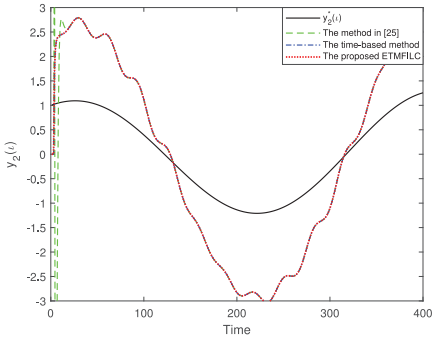

Fig. 14. $y_2(\iota)$ under three schemes for the 5th iteration.

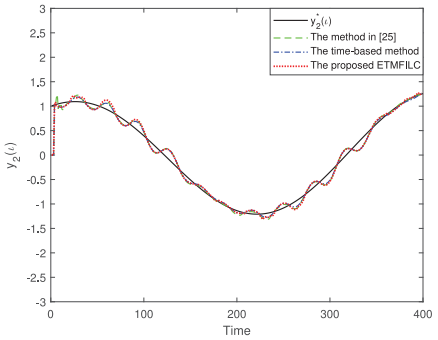

Fig. 15. $y_2(\iota)$ under three schemes for the 15th iteration.

TABLE II
COMPARISON OF TRANSMITTED TIMES FOR 50 ITERATIONS

	The proposed ETMFILC	The method in [25]
Transmission times	10164	10441

three specified instants. The comparison of transmission times is supplied in Table II.

According to Figs. 11–16, there is a tiny difference among the different methods after 50 iterations, so do the estimated uncertainties in Figs. 17 and 18. It is seen from Figs. 19 and 20 that the presented ETMFILC renders the smaller average error than [25]. Figs. 21–24 verify the validity of the proposed triggering mechanism for the MIMO case. Meanwhile, Table II conveys that the transmission times of the proposed ETMFILC is less than [25].

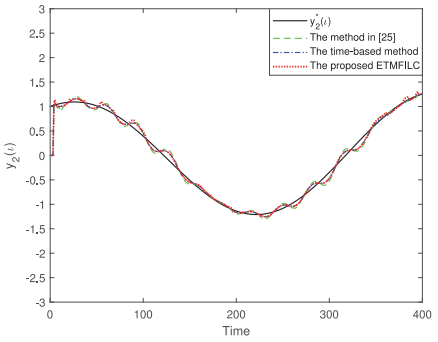

Fig. 16. $y_2(\iota)$ under three schemes for the 50th iteration.

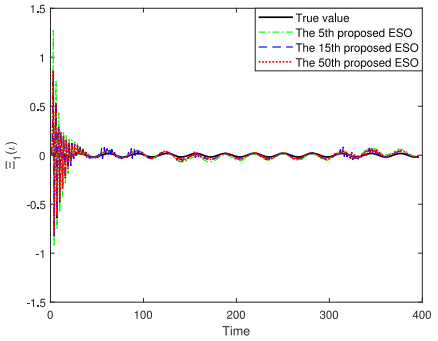

Fig. 17. Estimated $\Xi_1(\iota)$ for different iterations.

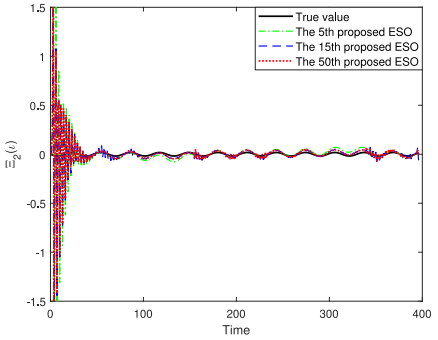

Fig. 18. Estimated $\Xi_2(\iota)$ for different iterations.

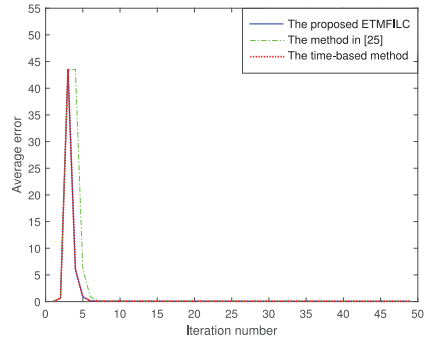

Fig. 19. Average errors of $y_1(\iota)$ with three schemes.

V. CONCLUSION

This article is dedicated to ETMFILC of nonlinear systems with disturbances. An output dynamic estimation method is constructed by the triggered output at triggering or itself during the interevent instants. Moreover, the estimated uncertainties

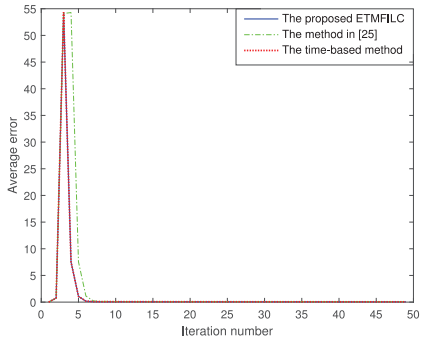

Fig. 20. Average errors of $y_2(\iota)$ with three schemes.

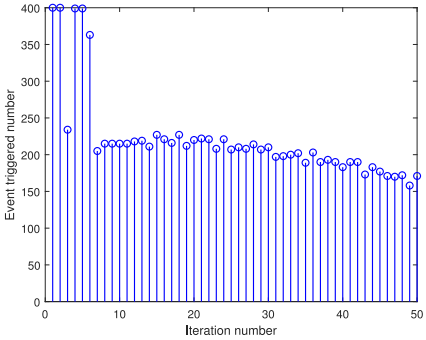

Fig. 21. Triggering number per iteration.

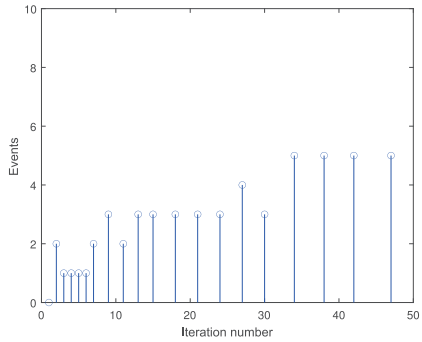

Fig. 22. Release events at $\iota = 50$.

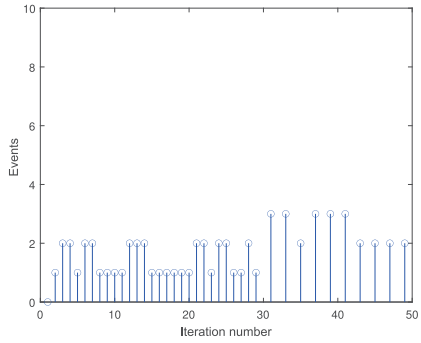

Fig. 23. Release events at $\iota = 150$.

are observed effectively by the improved ESO. The triggering conditions for SISO and MIMO systems are designed by utilizing the true tracking error, the estimated errors, and the estimated uncertainties, respectively. The uniformly ultimately bounded error systems are established for two types systems. Finally, illustrative examples are supplied to confirm

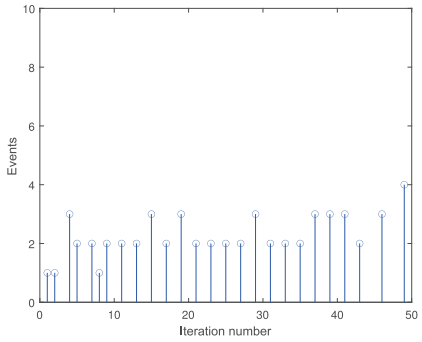

Fig. 24. Release events at $\iota = 340$.

the validity of the presented schemes. How to extend the proposed schemes with output quantization will be conducted in the future.

REFERENCES

[1] C. Peng, J. Wu, and E. Tian, "Stochastic event-triggered H_∞ control for networked systems under denial of service attacks," *IEEE Trans. Syst., Man, Cybern., Syst.*, vol. 52, no. 7, pp. 4200–4210, Jul. 2022.

[2] D.-W. Zhang, G.-P. Liu, and L. Cao, "Proportional integral predictive control of high-order fully actuated networked multiagent systems with communication delays," *IEEE Trans. Syst., Man, Cybern., Syst.*, early access, Jul. 14, 2022, doi: 10.1109/TSMC.2022.3188504.

[3] X. Du, X. Zhan, J. Wu, and H. Yan, "Performance analysis of MIMO information time-delay system under bandwidth, cyber-attack, and Gaussian white noise," *IEEE Trans. Syst., Man, Cybern., Syst.*, early access, Oct. 13, 2022, doi: 10.1109/TSMC.2022.3211620.

[4] X. Huang, J. Li, and Q. Su, "An observer with cooperative interaction structure for biasing attack detection and secure control," *IEEE Trans. Syst., Man, Cybern., Syst.*, early access, Oct. 20, 2022, doi: 10.1109/TSMC.2022.3213516.

[5] D. Ding, Q.-L. Han, X. Ge, and J. Wang, "Secure state estimation and control of cyber-physical systems: A survey," *IEEE Trans. Syst., Man, Cybern., Syst.*, vol. 51, no. 1, pp. 176–190, Jan. 2021.

[6] L. Shi, W. X. Zheng, J. Shao, and Y. Cheng, "Scaled tracking consensus in discrete-time second-order multiagent systems with random packet dropouts," *IEEE Trans. Syst., Man, Cybern., Syst.*, vol. 51, no. 12, pp. 7745–7751, Dec. 2021.

[7] D. K. Panda, S. Das, and S. Townley, "Toward a more renewable energy-based LFC under random packet transmissions and delays with stochastic generation and demand," *IEEE Trans. Autom. Sci. Eng.*, vol. 19, no. 2, pp. 1217–1232, Apr. 2022.

[8] M. M. Amiri and D. Gündüz, "Federated learning over wireless fading channels," *IEEE Trans. Wireless Commun.*, vol. 19, no. 5, pp. 3546–3557, May 2020.

[9] C. G. Cassandras, "The event-driven paradigm for control, communication and optimization," *J. Control Decis.*, vol. 1, pp. 3–17, Mar. 2014.

[10] C. Deng, W.-W. Che, and Z.-G. Wu, "A dynamic periodic event-triggered approach to consensus of heterogeneous linear multiagent systems with time-varying communication delays," *IEEE Trans. Cybern.*, vol. 51, no. 4, pp. 1812–1821, Apr. 2021.

[11] T. Li, D. Yang, X. Xie, and H. Zhang, "Event-triggered control of nonlinear discrete-time system with unknown dynamics based on HDP(λ)," *IEEE Trans. Cybern.*, vol. 52, no. 7, pp. 6046–6058, Jul. 2022, doi: 10.1109/TCYB.2020.3044595.

[12] K. Zhang, R. Su, H. Zhang, and Y. Tian, "Adaptive resilient event-triggered control design of autonomous vehicles with an iterative single critic learning framework," *IEEE Trans. Neural Netw. Learn. Syst.*, vol. 32, no. 12, pp. 5502–5511, Dec. 2021.

[13] P. Tabuada, "Event-triggered real-time scheduling of stabilizing control tasks," *IEEE Trans. Autom. Control*, vol. 52, no. 9, pp. 1680–1685, Sep. 2007.

[14] W. P. M. H. Heemels, M. C. F. Donkers, and A. R. Teel, "Periodic event-triggered control for linear systems," *IEEE Trans. Autom. Control*, vol. 58, no. 4, pp. 847–861, Apr. 2013.

[15] Z. Gu, P. Shi, D. Yue, and Z. Ding, "Decentralized adaptive event-triggered H_∞ filtering for a class of networked nonlinear interconnected systems," *IEEE Trans. Cybern.*, vol. 49, no. 5, pp. 1570–1579, May 2019.

[16] Z. Hou and S. Jin, "Data-driven model-free adaptive control for a class of MIMO nonlinear discrete-time systems," *IEEE Trans. Neural Netw.*, vol. 22, no. 12, pp. 2173–2188, Dec. 2011.
[17] J.-S. Wang and G.-H. Yang, "Data-driven methods for stealthy attacks on TCP/IP-based networked control systems equipped with attack detectors," *IEEE Trans. Cybern.*, vol. 49, no. 8, pp. 3020–3031, Aug. 2019.
[18] Z. Peng, L. Liu, and J. Wang, "Output-feedback flocking control of multiple autonomous surface vehicles based on data-driven adaptive extended state observers," *IEEE Trans. Cybern.*, vol. 51, no. 9, pp. 4611–4622, Sep. 2021.
[19] Q.-Y. Fan and G.-H. Yang, "Adaptive actor–critic design-based integral sliding-mode control for partially unknown nonlinear systems with input disturbances," *IEEE Trans. Neural Netw. Learn. Syst.*, vol. 27, no. 1, pp. 165–177, Jan. 2016.
[20] G. Bontempi, M. Birattari, and H. Bersini, "Lazy learning for local modelling and control design," *Int. J. Control*, vol. 72, pp. 643–658, Nov. 2010.
[21] Z. Hou and S. Jin, "A novel data-driven control approach for a class of discrete-time nonlinear systems," *IEEE Trans. Control Syst. Technol.*, vol. 19, no. 6, pp. 1549–1558, Nov. 2011.
[22] Z. Hou, R. Chi, and H. Gao, "An overview of dynamic-linearization-based data-driven control and applications," *IEEE Trans. Ind. Electron.*, vol. 64, no. 5, pp. 4076–4090, May 2017.
[23] Y.-S. Ma, W.-W. Che, C. Deng, and Z.-G. Wu, "Observer-based event-triggered containment control for MASs under DoS attacks," *IEEE Trans. Cybern.*, vol. 52, no. 12, pp. 13156–13167, Dec. 2022, doi: 10.1109/TCYB.2021.3104178.
[24] N. Lin, R. Chi, and B. Huang, "Event-triggered model-free adaptive control," *IEEE Trans. Syst., Man, Cybern., Syst.*, vol. 51, no. 6, pp. 3358–3369, Jun. 2021.
[25] N. Lin, R. Chi, B. Huang, and Z. Hou, "Event-triggered nonlinear iterative learning control," *IEEE Trans. Neural Netw. Learn. Syst.*, vol. 32, no. 11, pp. 5118–5128, Nov. 2021.
[26] N. Lin, R. Chi, and B. Huang, "Event-triggered ILC for optimal consensus at specified data points of heterogeneous networked agents with switching topologies," *IEEE Trans. Cybern.*, vol. 52, no. 9, pp. 8951–8961, Sep. 2022, doi: 10.1109/TCYB.2021.3054421.
[27] D. Liu and G.-H. Yang, "Neural network-based event-triggered MFAC for nonlinear discrete-time processes," *Neurocomputing*, vol. 272, pp. 356–364, Jan. 2018.
[28] X. Bu, Z. Hou, F. Yu, and Z. Fu, "Model free adaptive control with disturbance observer," *J. Control Eng. Appl. Inform.*, vol. 14, no. 4, pp. 42–49, 2012.
[29] H.-F. Li, Y.-C. Wang, and H.-G. Zhang, "Data-driven-based event-triggered tracking control for non-linear systems with unknown disturbance," *IET Control Theory Appl.*, vol. 13, pp. 2197–2206, Sep. 2019.
[30] R. Chi, Y. Hui, B. Huang, and Z. Hou, "Active disturbance rejection control for nonaffined globally Lipschitz nonlinear discrete-time systems," *IEEE Trans. Autom. Control*, vol. 66, no. 12, pp. 5955–5967, Dec. 2021.
[31] V. Utkin, "Chattering problem," *IFAC Proc. Vol.*, vol. 44, pp. 13374–13379, Jan. 2011.
[32] Y. Xu, F. Jia, C. Ma, J. Mao, and S. Zhang, "Chatter free sliding mode control of a chaotic coal mine power grid with small energy inputs," *Int. J. Min. Sci. Technol.*, vol. 22, pp. 477–481, Jul. 2012.
[33] J. M. Ortega and W. C. Rheinboldt, *Iterative Solution of Nonlinear Equations in Several Variables*. Philadelphia, PA, USA: Soc. Ind. Appl. Math., 2000.
[34] S. Gerschgorin, "Uber die abgrenzung der Eigenwerte einer matrix," *Izvestija Akademii Nauk SSSR, Serija Matematika*, vol. 7, no. 3, pp. 749–754, 1931.
[35] D. Meng and K. L. Moore, "Robust iterative learning control for non-repetitive uncertain systems," *IEEE Trans. Autom. Control*, vol. 62, no. 2, pp. 907–913, Feb. 2017.

Mouquan Shen received the Ph.D. degree in control theory and control engineering from the College of Information Science and Engineering, Northeastern University, Shenyang, China, in 2011.

He is with the College of Electrical Engineering and Control Science, Nanjing Tech University, Nanjing, China. He is also with the Department of Electrical Engineering, Yeungnam University, Kyonsan, Republic of Korea. His current research interests include Markov jump systems, adaptive control, data-driven-based control, robust control, and interactive learning control.

Xianming Wang received the B.S. degree in measurement control technology and instruments from the College of Electrical Engineering and Control Science, Nanjing Tech University, Nanjing, China, where he is currently pursuing the Ph.D. degree in power engineering and engineering thermophysics.

His current research interests include data-driven control, event-triggered control, and adaptive dynamic programming.

Ju H. Park (Senior Member, IEEE) received the Ph.D. degree in electronics and electrical engineering from the Pohang University of Science and Technology (POSTECH), Pohang, Republic of Korea, in 1997.

From 1997 to 2000, he was a Research Associate with the Engineering Research Center-Automation Research Center, POSTECH. He joined Yeungnam University, Kyongsan, Republic of Korea, in 2000, where he is currently the Chuma Chair Professor. He is a coauthor of the monographs *Recent Advances in Control and Filtering of Dynamic Systems With Constrained Signals* (Springer-Nature, 2018) and *Dynamic Systems With Time Delays: Stability and Control* (Springer-Nature, 2019) and an Editor of an edited volume *Recent Advances in Control Problems of Dynamical Systems and Networks* (Springer-Nature, 2020). His research interests include robust control and filtering, neural/complex networks, fuzzy systems, multiagent systems, and chaotic systems. He has authored or coauthored a number of articles in these areas.

Dr. Park has been a recipient of the Highly Cited Researchers Award by Clarivate Analytics (formerly, Thomson Reuters) since 2015 and was listed in three fields, Engineering, Computer Sciences, and Mathematics, from 2019 to 2022. He is also an Editor of the *International Journal of Control, Automation and Systems*. He is also a Subject Editor/Advisory Editor/Associate Editor/Editorial Board Member for several international journals, including *IET Control Theory and Applications*, *Applied Mathematics and Computation*, *Journal of the Franklin Institute*, *Nonlinear Dynamics*, *Engineering Reports*, *Cogent Engineering*, IEEE TRANSACTION ON FUZZY SYSTEMS, IEEE TRANSACTIONS ON NEURAL NETWORKS AND LEARNING SYSTEMS, and IEEE TRANSACTIONS ON CYBERNETICS. He is a Fellow of the Korean Academy of Science and Technology, Gyeonggi, Republic of Korea.

Yang Yi received the M.Sc. degree in information engineering from Yangzhou University, Yangzhou, China, in 2005, and the Ph.D. degree in automation from Southeast University, Nanjing, China, in 2009.

He is currently a Professor with the College of Information Engineering, Yangzhou University. From 2012 to 2013, he was a Visiting Scientist with the School of Computing, Engineering and Mathematics, University of Western Sydney, Penrith, NSW, Australia. He has published more than 60 papers in journals and conferences. His current research interests include stochastic systems, intelligent systems, and anti-disturbance control.

Wei-Wei Che received the B.S. degree in mathematics and applied mathematics from Jinzhou Normal University, Jinzhou, China, in 2002, the M.S. degree in applied mathematics from Bohai University, Jinzhou, in 2005, and the Ph.D. degree in control engineering from Northeastern University, Shenyang, China, in 2008.

She was a Postdoctoral Fellow with the IEEE, Nanyang Technological University, Singapore, from 2008 to 2009. She was a Research Associate with the Department of Mechanical Engineering, University of Hong Kong, Hong Kong, in 2015. She is currently a Professor with the Institute of System Science, Qingdao University, Qingdao, China. Her research interests include nonfragile control, quantization control, as well as fault-tolerant control and their applications to NCSs, MASs, and CPSs design.